Longitudinal Lorentz force on a subwavelength-diameter optical fiber

Huakang Yu,[1] Wei Fang,[1,*] Fuxing Gu,[1] Min Qiu,[1,2] Zongyin Yang,[1] and Limin Tong[1,†]

[1]*State Key Laboratory of Modern Optical Instrumentation, Department of Optical Engineering, Zhejiang University, Hangzhou 310027, China*

[2]*Department of Microelectronics and Applied Physics, Royal Institute of Technology (KTH), Electrum 229, 164 40 Kista, Sweden*

(Received 21 January 2011; published 20 May 2011)

We analyze the longitudinal Lorentz forces that a propagating continuous-wave light exerts on a subwavelength-diameter optical fiber. Our theoretical results show that, during the propagating process, the guided light exerts no net time-averaged force on the fiber. Via numerical simulation, we find a significant overall pull force of 0.4 pN/mW acting on a 450-nm-diam fiber tip at a wavelength of 980 nm due to the scattering of the end face and a calculated force distribution reveals the feature of a near-field accumulation. Our results may be helpful to the configuration of optomechanical components or devices based on these fibers.

DOI: 10.1103/PhysRevA.83.053830 PACS number(s): 42.50.Wk, 03.50.De

I. INTRODUCTION

Though the electromagnetic stress tensor, i.e., the Maxwell stress tensor, in free space is readily derived from the Lorentz force law and Maxwell equations, the form of the stress tensor inside media [1,2] has been debated over the past century. The Minkowski form predicts the single-photon momentum in a medium as $\boldsymbol{p}_{\mathrm{Min}} = n\boldsymbol{p}_0$, while the Abraham form is $\boldsymbol{p}_{\mathrm{Abr}} = \boldsymbol{p}_0/n$, where $\boldsymbol{p}_0 = \hbar\boldsymbol{k}_0$ is the single-photon momentum in free space and n represents the refractive index of the medium. Extensive theoretical and experimental work has been carried out attempting to solve the Minkowski-Abraham dilemma (a brief review of this problem can be found in Refs. [3,4]). Most recently, Barnett announced the resolution of the Abraham-Minkowski dilemma in Ref. [5], where the author showed that both the Minkowski and Abraham forms were correct, with Minkowski's denoting the canonical momentum and Abraham's denoting the kinetic momentum. While deriving the stress tensor seems difficult and complicated in a specific case, the Lorentz force combined with the Maxwell equations, however, can be directly applied to provide the optical force distribution throughout the medium. This method's generality has been shown to be advantageous in various applications, especially in solid metals and dielectrics without involving the Abraham-Minkowski dilemma [6,7], and its equivalence to Maxwell's stress tensor analysis has also been demonstrated [8]. Moreover, the direct computations of the Lorentz force with bound charges and currents are applicable to the finite-difference time domain (FDTD) numerical simulation method throughout the medium while showing the feasibility of applying this method to various situations of interest [9].

Despite numerous theoretic arguments attempting to resolve the debate, only a few experiments have been performed to test the theory (see Refs. [3–5] for a brief review). Recently She *et al.* [10] carried out an experiment in which a continuous-wave (CW) laser was launched into a free-suspending subwavelength-diameter (SD) silica optical fiber. By observing the response of the free fiber end, the authors suggested that a push force was exerted by the outgoing light on the end face of the fiber. Thus they concluded that the Abraham momentum inside the medium is correct. The experiment seems rather simple, but its conclusion was questioned by Mansuripur and Zakharian [11–13] and Brevik and Ellingsen [14,15].

In Mansuripur and Zakharian's opinion [11–13], the theoretic interpretation in the work of She *et al.* should be more carefully considered. Mansuripur and Zakharian numerically investigated the momentum change at the fiber tip by calculating the impulse (brought in by a 10-fs light pulse) via a FDTD method [12], which yielded an overall pull force (rather than a push force). Their work gave better physical insight into this problem. It should be pointed out that in the experiment of She *et al.* a CW laser was used (though it was chopped into pulses in some cases, the pulse duration was on the order of seconds). Thus it would be more interesting to study the case of CW light.

Brevik and Ellingsen proposed a different mechanism [15] to explain what had been observed by She *et al.* By introducing a slight axial asymmetry of the transverse refractive index n distribution that might come from the fabrication process, light propagation along the SD fiber could produce a net transverse surface force density and thus cause observable sideways displacement of the fiber tip. However, the longitudinal Lorentz force analysis was not included in this study even though its effects may not be ignored in the experiment of She *et al.* due to the existence of the end face.

As a complement, in this paper we present our theoretical and numerical simulation studies on the longitudinal Lorentz force that a propagating CW light exerts on a free-suspending SD fiber and its end face. Moreover, though the explanations and conclusions of She *et al.* have been questioned, the SD fiber used in the experiment is a promising tool to study nanoscale optomechanics, which benefits from favorable properties including excellent uniformity [16], low propagation loss, tight optical confinement, and strong evanescent field, as indicated in Ref. [17]. Thus a clear understanding of the longitudinal Lorentz force acting on the SD fiber is necessary in optomechanics, especially in the case of CW light.

The paper is organized as follows. In Sec. II we describe the analysis of longitudinal forces on a SD fiber for the fundamental mode. Section III gives detailed FDTD numerical

*wfang08@zju.edu.cn
†phytong@zju.edu.cn

simulation results of the light scattering at the SD fiber end and the longitudinal Lorentz force is computed. Finally, a summary of our conclusions is presented in Sec. IV.

II. LONGITUDINAL LORENTZ FORCES ON AN INFINITELY LONG SD FIBER

In the experiment of She *et al.*, a 980-nm laser was launched into a 450-nm-diam SD fiber that supports only the fundamental mode. To imitate the work of She *et al.*, here we investigate the case of CW light propagation along an infinitely long lossless single-mode SD fiber with circular cross section and uniform diameter. The nonlinear optical effects have not been taken into account in our study. The CW treatment we present in this work is compatible with the experiment of She *et al.*, as shown previously. During the propagation, the instantaneous Lorentz force density that the electromagnetic field exerts on the media is given by [18]

$$\boldsymbol{f} = \rho_b \boldsymbol{E} + \boldsymbol{J}_b \times \mu_0 \boldsymbol{H} = -(\nabla \cdot \boldsymbol{P})\boldsymbol{E} + \frac{\partial \boldsymbol{P}}{\partial t} \times \mu_0 \boldsymbol{H}, \quad (1)$$

where $\boldsymbol{E}$ and $\boldsymbol{H}$ are the electric and magnetic fields of the optical mode in the fiber, respectively, ρ_b is the bound charge density, $\boldsymbol{J}_b$ is the bound current density, $\boldsymbol{P}$ is the electric polarization density, and μ_0 is the permeability of vacuum. Because the longitudinal (i.e., the z direction in this paper) force is of the most interest here, we focus only on the Lorentz force density along the longitudinal direction:

$$\boldsymbol{f}_z = \rho_b \boldsymbol{E}_z + (\boldsymbol{J}_b \times \mu_0 \boldsymbol{H})_z. \quad (2)$$

Note that the fibers used in the experiments of She *et al.* were under single-mode operation, so here we include only the fundamental optical mode (HE_{11}) of the fiber in the calculation. We have the electric- and magnetic-field components [19]

$$\boldsymbol{E}_t = E_t \cos(\beta z - \omega t)\hat{\boldsymbol{t}} = (E_r \hat{\boldsymbol{r}} + E_\varphi \hat{\boldsymbol{\varphi}}) \cos(\beta z - \omega t), \quad (3)$$

$$\boldsymbol{H}_t = H_t \cos(\beta z - \omega t)\hat{\boldsymbol{t}} = (H_r \hat{\boldsymbol{r}} + H_\varphi \hat{\boldsymbol{\varphi}}) \cos(\beta z - \omega t), \quad (4)$$

$$\boldsymbol{E}_z = E_z \sin(\beta z - \omega t)\hat{\boldsymbol{z}}, \quad (5)$$

$$\boldsymbol{H}_z = H_z \sin(\beta z - \omega t)\hat{\boldsymbol{z}}, \quad (6)$$

$$\boldsymbol{P} = \epsilon_0(\epsilon_r - 1)\boldsymbol{E}, \quad (7)$$

where $\hat{\boldsymbol{t}}$, $\hat{\boldsymbol{z}}$, $\hat{\boldsymbol{r}}$, and $\hat{\boldsymbol{\varphi}}$ are unit vector along transverse, longitudinal, radial, and azimuthal directions, respectively; $\boldsymbol{E}_t(\boldsymbol{H}_t)$, $\boldsymbol{E}_z(\boldsymbol{H}_z)$, $\boldsymbol{E}_r(\boldsymbol{H}_r)$, and $\boldsymbol{E}_\varphi(\boldsymbol{H}_\varphi)$ are the transverse, longitudinal, radial, and azimuthal electric (magnetic) fields, respectively; β is the propagation constant; ω is the angular frequency of the field; and ϵ_0 and ϵ_r are the permittivity of the vacuum and the relative permittivity, respectively. With Eqs. (2)–(7), the instantaneous longitudinal Lorentz force density becomes

$$\boldsymbol{f}_z = \frac{\epsilon_0(\epsilon_r - 1)}{2}\left[\left(E_z \frac{\partial}{\partial r} E_r + E_z \frac{1}{r}\frac{\partial}{\partial \varphi} E_\varphi + \beta E_z^2\right) + \mu_0 \omega (E_r H_\varphi - H_r E_\varphi)\right] \sin 2(\beta z - \omega t)\hat{\boldsymbol{z}}. \quad (8)$$

For a SD silica fiber with a diameter of 450 nm, a refractive index of 1.45, and an incident light with a wavelength at 980 nm, we substitute the electric- and magnetic-field expressions of the HE_{11} mode (from Ref. [19]) into Eq. (8). Then we integrate $\boldsymbol{f}_z$ over the transverse cross-sectional plane, that is, $\boldsymbol{F}_z = \int\int \boldsymbol{f}_z d\sigma$. Finally, we have the instantaneous longitudinal force distribution as a function of z [as shown in Fig. 1 solid line)], which demonstrates a spatial oscillation with a period of $2\pi/2\beta$. The calculated amplitude is 9.7 pN/μm mW, which is considerably large for microscale or nanoscale devices [17].

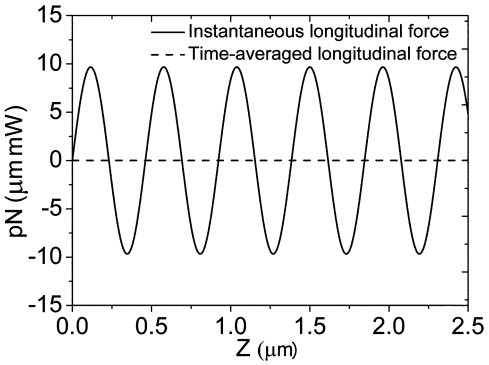

FIG. 1. The solid line shows the instantaneous longitudinal force distribution as a function of z for a typical SD silica fiber with a diameter of 450 nm and incident light with a wavelength of 980 nm. The dashed line shows the time-averaged longitudinal force.

The total time-averaged longitudinal force can be obtained by integration over one optical period T,

$$\langle \boldsymbol{F}_z \rangle = \frac{1}{T}\int_0^T dt \int\int \boldsymbol{f}_z d\sigma. \quad (9)$$

Clearly, the total time-averaged longitudinal force density $\langle \boldsymbol{F}_z \rangle$ inside the fiber vanishes, i.e., $\langle \boldsymbol{F}_z \rangle = 0$ for the fundamental mode, as shown in Fig. 1 (dashed line). The same results can be obtained for higher-order modes propagating inside the SD fiber.

These results are understandable. While light propagates inside a medium, the interaction between the light and the medium is accompanied by a momentum exchange and the part obtained by the medium is mechanical momentum. The same happens here in the SD fiber: While integrating over one period, the net impulse that the medium gains is zero, which means that there is no momentum or energy loss for the CW light of a stationary mode in a homogeneous and transparent medium.

III. LONGITUDINAL LORENTZ FORCE ON A SD FIBER END

Practically, and in most experimental cases, the SD fiber should have an end. When light arrives at the free end face of a SD fiber, it will encounter scattering, i.e., reflection and diffraction, due to the abrupt interface. Unlike the bulk material, the situation in SD fibers shows significantly different properties [20,21], especially due to the tight confinement accompanied by a large fractional evanescent wave propagating outside the fiber. As schematically shown in Fig. 2(a), the scattered output can be roughly divided into two parts at the plane of the fiber end face, i.e., the light reflected back

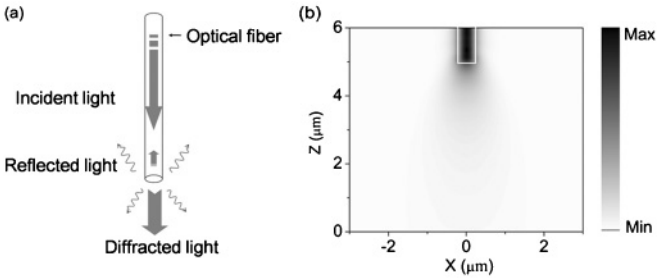

FIG. 2. (a) Schematic of the reflected and diffracted light at the end face of the SD fiber. (b) Calculated z-direction Poynting vector distribution in the x-z ($y = 0$) cross-sectional plane for a 450-nm-diam silica fiber with a refractive index of 1.45 at a wavelength of 980 nm (quasi-x-polarized). The white line represents the profile of the fiber.

into the upper half-space or diffracted forward into the lower half-space. Considering that the waveguided light cannot be treated simply as a plane wave, an analytical solution is difficult to obtain. Here we refer to numerical simulation using a three-dimensional FDTD method to investigate light output features. A flat-ended 450-nm-diam silica fiber and a CW light source with a wavelength of 980 nm are used in our simulation. The total simulation region is $10 \times 10 \times 8\ \mu\text{m}^3$ with a cell size of 20 nm and terminated by a perfectly matched layer (PML) boundary condition. The calculated distribution of the z-direction Poynting vector in the x-z ($y = 0$) cross-sectional plane is shown in Fig. 2(b). The measured fractional power of light in the z direction is 92% across a plane 5.5 μm away from the output end face due to diffraction. At the same time, part of total incident power (∼1%) reflects into the upper half-space at the end face, as indicated in Fig. 2(a). Part of the reflected light will propagate along the direction opposite the incident light in the guided mode, while the rest transmits to free space in the radiated mode.

To study the Lorentz force on the SD fiber, a quasi-x-polarized CW light with a wavelength of 980 nm is used. The length of the fiber chosen for simulation is 9.5 μm and the total region terminated by the PML boundary condition is $2 \times 2 \times 10\ \mu\text{m}^3$ with a cell size of 20 nm. Figure 3(a) shows the computed instantaneous profile of E_x on the x-z ($y = 0$) cross-sectional plane.

To calculate the Lorentz force density along the longitudinal direction, we first calculate the bound charge and bound current densities by following the method indicated in Ref. [9] and then compute the instantaneous force density $\boldsymbol{f}_z$ using Eq. (2). The bound charge exists only on the surface of the SD fiber, while the bound current exists everywhere inside the fiber. The time-averaged longitudinal Lorentz force density over the transverse cross-sectional plane, $\langle \boldsymbol{F}_z \rangle = \frac{1}{T} \int_0^T dt \int\int \boldsymbol{f}_z dx\, dy$, is plotted in Fig. 3(b) as a function of z. Different from the case of an infinitely long SD fiber where the time-averaged force vanishes (dashed line in Fig. 1), an oscillation is shown with a period of π/β. Such an oscillation results from the interference between the incident wave and the reflected wave; similar behavior is also present in a dielectric slab illuminated at normal incidence by a plane wave [6] (for more details, see the Appendix). However, due to the finite size of the fiber end face, a fraction

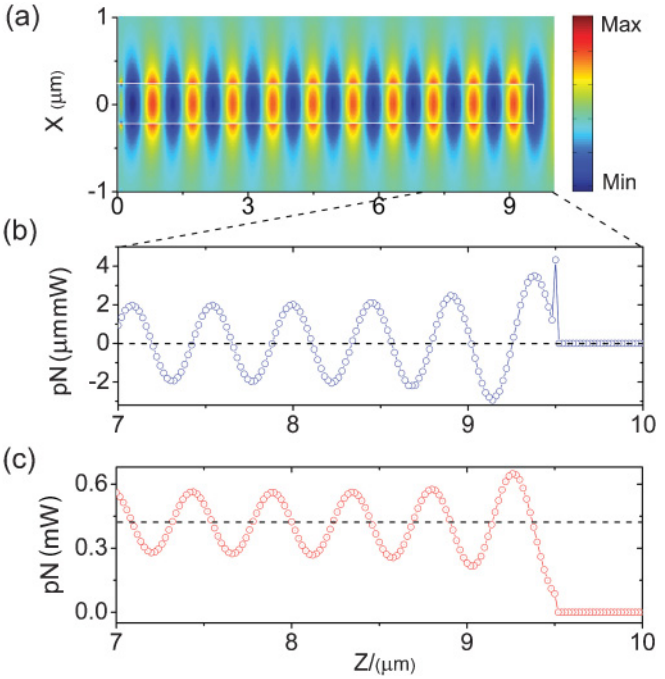

FIG. 3. (Color online) (a) Computed instantaneous E_x distribution on the x-z ($y = 0$) cross-sectional plane. The white line represents the profile of the fiber. (b) Time-averaged Lorentz force over the transverse cross-sectional plane F_z as a function of z. (c) Integrated F_z from the fiber end face to a position where $z < 9.5\ \mu$m.

of the reflected light escapes from the fiber into the free space in the radiated mode. Thus the amplitude of the oscillation decreases with distance away from the end face and stabilizes after several periods. Another phenomenon that is different from the slab case mentioned above is the $\langle \boldsymbol{F}_z \rangle$ discontinuity at the fiber end face, as shown in Fig. 3(b). Recall that in homogeneous media, the bound charge exists only on the surface, while the interface is treated as a layer with a finite thickness of 20 nm in the FDTD code. With a nonzero E_z component of the HE_{11} mode, we get a time-averaged pull force of 96 fN/mW from the bound charge contribution on the end face layer, while the contribution from the bound current is a much smaller push force of 8.8 fN/mW from the same layer. To show the surface effect on Fig. 3(b), we divided the total force by the thickness of the surface layer to get an average force density.

After integrating $\langle \boldsymbol{F}_z \rangle$ along the z axis from the fiber end face ($z = 9.5\ \mu$m) into the fiber, that is, $\int_{z=9.5\,\mu\text{m}}^{z=Z\,(Z<9.5\,\mu\text{m})} \langle \boldsymbol{F}_z \rangle dz$, we obtain an oscillating overall pull force, shown in Fig. 3(c). While the oscillation stabilizes ($z < 8\ \mu$m), we get an average value of 0.4 pN/mW [as depicted by the dashed line in Fig. 3(c)] exerted on the fiber tip. This overall pull force is obtained not solely from the force caused by the surface charge or current as discussed above (shown as a small gap at $z = 9.5\ \mu$m), but by the force accumulating over the near-field region close to the end face, where the radiated mode escapes from the fiber. With an incident light power of 1 mW, the magnitude of the pull force is comparable with the weight of a 10-μm-long SD silica fiber 450 nm in diameter.

Regarding the experiment conducted by She *et al.*, the situation is more complicated. Initially, a small bending at the tip or a tilted end face will introduce a transversal force component, which, combined with the transversal force indicated by Brevik and Ellingsen [15] and other effects, may act on the fiber tip to have a considerable impact and contribute to the deformations.

IV. CONCLUSION

We have analyzed longitudinal Lorentz forces of a guided CW light on a SD fiber and the fiber tip. The present results suggest that, during the propagation, the fundamental optical mode exerts no net force on the fiber by means of time averaging. After careful calculation of optical forces on the fiber tip via numerical method, an overall pull force of 0.4 pN/mW is obtained, due to scattering on the fiber end face. Our results may be helpful in the configuration of optomechanical components or devices based on these fibers, such as all-optical switches [22].

ACKNOWLEDGMENTS

The authors gratefully thank M. Sumetsky and J. Fu for valuable discussions. This work was supported by the National Basic Research Programs of China (Grant No. 2007CB307003) and the National Natural Science Foundation of China (Grants No. 10974178 and No. 60907036).

APPENDIX

The reflected optical mode should have electric- and magnetic-field components:

$$\begin{aligned}\boldsymbol{E}_{t,r} &= \rho E_t \cos(-\beta z - \omega t - \Delta\varphi)\hat{\boldsymbol{t}} \\ &= \rho(E_r\hat{\boldsymbol{r}} + E_\varphi\hat{\boldsymbol{\varphi}})\cos(-\beta z - \omega t - \Delta\varphi), \end{aligned} \tag{A1}$$

$$\begin{aligned}\boldsymbol{H}_{t,r} &= -\rho H_t \cos(-\beta z - \omega t - \Delta\varphi)\hat{\boldsymbol{t}} \\ &= -\rho(H_r\hat{\boldsymbol{r}} + H_\varphi\hat{\boldsymbol{\varphi}})\cos(-\beta z - \omega t - \Delta\varphi), \end{aligned} \tag{A2}$$

$$\boldsymbol{E}_{z,r} = -\rho E_z \sin(-\beta z - \omega t - \Delta\varphi)\hat{\boldsymbol{z}}, \tag{A3}$$

$$\boldsymbol{H}_{z,r} = -\rho H_z \sin(-\beta z - \omega t - \Delta\varphi)\hat{\boldsymbol{z}}, \tag{A4}$$

where ρ represents the reflectivity and $\Delta\varphi$ is the abrupt phase change of reflected light at the end face. Now we can obtain the total electric and magnetic fields using Eqs. (3)–(6) and (A1)–(A4); thus the time-averaged longitudinal Lorentz force density becomes

$$\begin{aligned}\langle \boldsymbol{f}_z \rangle = \frac{\epsilon_0(\epsilon_r - 1)\rho}{T}\Bigg[\left(E_z\frac{\partial}{\partial r}E_r + E_z\frac{1}{r}\frac{\partial}{\partial\varphi}E_\varphi + \beta E_z^2\right) \\ +\mu_0\omega(H_r E_\varphi - E_r H_\varphi)\Bigg]\sin(2\beta z + \Delta\varphi)\hat{\boldsymbol{z}}. \end{aligned} \tag{A5}$$

It is clear that the time-averaged longitudinal Lorentz force would experience a 2β-periodic sinusoidal variation as a function of z because the reflected optical mode interferes with the guided incident light.

[1] H. Minkowski, Nachr. Kön. Ges. Wiss. Göttingen Math.-Phys. Kl.53 (1908).
[2] M. Abraham, Rend. Circ. Mat. Palermo **28**, 1 (1909).
[3] I. Brevik, Phys. Rep. **52**, 133 (1979).
[4] R. N. C. Pfeifer, T. A. Nieminen, N. R. Heckenberg, and H. Rubinsztein-Dunlop, Rev. Mod. Phys. **79**, 1197 (2007).
[5] S. M. Barnett, Phys. Rev. Lett. **104**, 070401 (2010).
[6] M. Mansuripur, Opt. Express **12**, 5375 (2004).
[7] R. Loudon and S. M. Barnett, Opt. Express **14**, 11855 (2006).
[8] B. A. Kemp, T. M. Grzegorczyk, and J. A. Kong, Opt. Express **13**, 9280 (2005).
[9] A. R. Zakharian, M. Mansuripur, and J. V. Moloney, Opt. Express **13**, 2321 (2005).
[10] W. L. She, J. H. Yu, and R. H. Feng, Phys. Rev. Lett. **101**, 243601 (2008).
[11] M. Mansuripur, Phys. Rev. Lett. **103**, 019301 (2009).
[12] M. Mansuripur and A. R. Zakharian, Phys. Rev. A **80**, 023823 (2009).
[13] M. Mansuripur and A. R. Zakharian, Phys. Rev. E **79**, 026608 (2009).
[14] I. Brevik, Phys. Rev. Lett. **103**, 219301 (2009).
[15] I. Brevik and S. A. Ellingsen, Phys. Rev. A **81**, 011806 (2010).
[16] L. M. Tong, R. R. Gattass, J. B. Ashcom, S. He, J. Lou, M. Shen, I. Maxwell, and E. Mazur, Nature (London) **426**, 816 (2003).
[17] D. V. Thourhout and J. Roels, Nature Photon. **4**, 211 (2010).
[18] J. D. Jackson, *Classical Electrodynamics* (Wiley, New York, 1999).
[19] A. W. Snyder and J. D. Love, *Optical Waveguide Theory* (Chapman and Hall, New York, 1983).
[20] S. S. Wang, Z. F. Hu, H. K. Yu, W. Fang, M. Qiu, and L. M. Tong, Opt. Express **17**, 10881 (2009).
[21] S. S. Wang, J. Fu, M. Qiu, K. J. Huang, Z. Ma, and L. M. Tong, Opt. Express **16**, 8887 (2008).
[22] J. H. Yu, R. H. Feng, and W. L. She, Opt. Express **17**, 4640 (2009).